ISSN 1845–8319

DYNAMICS OF THE CHROMOSPHERIC PLASMA OBSERVED BY *RHESSI*

T. MROZEK and S. KOŁOMAŃSKI

Astronomical Institute, University of Wrocław, ul. Kopernika 11, 51-622 Wrocław, Poland

Abstract. Good temporal and spectral resolution of *RHESSI* images gave us opportunity to investigate the chromospheric evaporation at several levels of the chromosphere. We performed such an analysis for a strong solar flare, with the use of images and spectra obtained by *RHESSI*. The altitudes of footpoint hard X-ray sources in various energy bands have been measured. We obtained the energy-height relation in several consecutive time intervals. Observed temporal evolution of the energy-height relation can be interpreted as manifestation of the chromospheric evaporation.

Key words: solar flares - footpoints - hard X-rays - chromospheric evaporation

1. Introduction

During the impulsive phase of a solar flare electrons are accelerated high in the solar corona. After escaping from the acceleration region, a part of them propagates along magnetic field lines and reaches the chromosphere where they deposit their energy due to Coulomb collisions. During this process we observe the hard X-ray bremsstrahlung and the thermal reaction of plasma in soft X-rays, UV and white light. Theoretical models (Nagai and Emslie, 1984; Fisher *et al.*, 1985) of the impulsive phase of a solar flare predict that the energy deposited in the chromosphere by non-thermal electron beam leads to high pressure gradients. This process is the main cause of the chromospheric evaporation.

The evaporation can be revealed with the use of several observables. Spectroscopic observations in lines which are produced in the low corona, transition region and chromosphere are most often used. The analysis of line profile asymmetries shows (Li *et al.*, 2006 and references within) that during impulsive phase plasma moves upward inside a magnetic loop with velocities of order of hundreds of km s^{-1}. Moreover, chromospheric evaporation was

observed with the use of the impulsive SXR brightenings occurring due to non-thermal electron beams (Tomczak, 1999; Mrozek and Tomczak, 2004). There is a clear relationship observed within the footpoint – the level located higher in the magnetic structure shows the maximum of the impulsive SXR brightening later in time. Assuming that this effect is directly related to the evaporation process, velocities of the evaporation can be calculated.

Mentioned observations of the chromospheric response to the non-thermal electron beam are based on the thermal emission of heated footpoint plasma. The hard X-ray bremsstrahlung produced directly due to the Coulomb collisions between non-thermal electrons and ambient plasma is the more basic signature of the non-thermal electron beam. The thick-target model (Brown, 1973) predicts that a relation between the energy of hard X-ray sources and their positions along the flux tube should be observed. We call it *the energy-height relation*. Such effect was observed by *Yohkoh* (Matsushita *et al.*, 1992) and recently by *RHESSI* (Aschwanden *et al.*, 2002; Mrozek, 2006). This relation may be very useful for investigating the non-thermal electrons precipitation at different levels of the chromosphere.

In this paper we present a new method of the chromospheric evaporation analysis. It is based on the temporal evolution of the energy-height relation. The method was applied to the flare of 3 Aug 2002, well observed by *RHESSI*.

2. Observations and Analysis

In our analysis we used data from *RHESSI* satellite (Lin et. al 2002). We chose a strong flare located near the solar limb for minimizing the projection effect. The impulsive phase of the flare was well observed by *RHESSI* and the footpoints were clearly seen. Moreover, this event was observed also by *TRACE* (Handy *et al.*, 1999) and EIT (Delaboudiniére *et al.*, 1996). Images taken with the use of these instruments were helpful in morphology verification.

We chose six consecutive, 12 s long time intervals covering the strongest hard X-ray burst (Figure 1). For each time interval we made images, using the CLEAN algorithm (Högbom, 1974), in different energy ranges with intervals changing from 2 keV to 20 keV in dependence of photon counts statistic. The shift between neighbouring ranges was equal to the half of their energy range length. This gave us ranges which had small influence

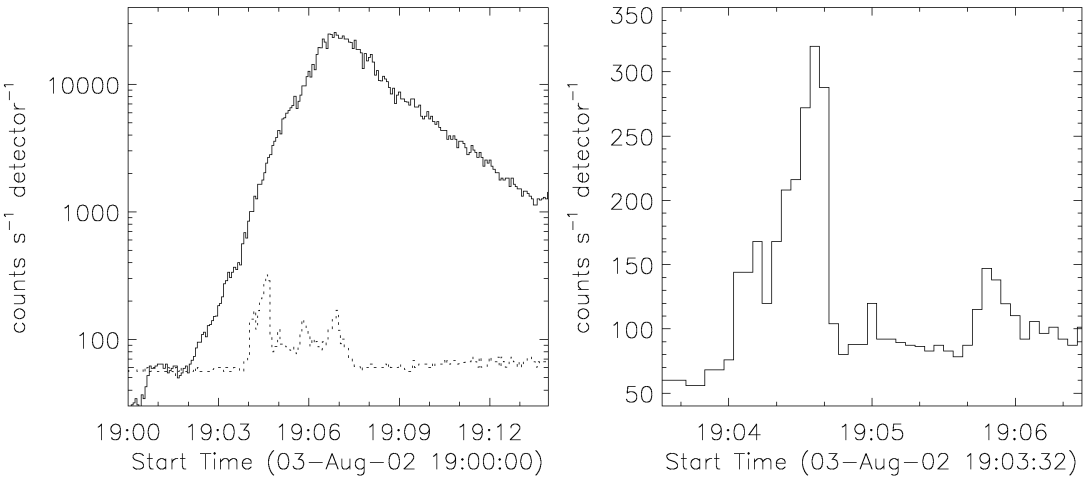

Figure 1: Left panel: Light curves of the 3 Aug 2002 flare obtained in two energy ranges: 6-12 keV (solid line) and 50-100 keV (dotted line). Right panel: Magnified 50-100 keV light curve of the first HXR peak.

from neighbouring intervals and could be treated as almost independent. Used energy ranges are presented in the Figure 3 (left panel) as horizontal lines.

The set of images obtained in different energy ranges and different time intervals was used for the further analysis. For each footpoint we determined the location of its centroid and measured its distance from the reference level. The level is defined by centroids obtained for the highest energy range (see Figure 2). The reference level is time independent, i.e. for each time interval it is located in the same position. Selected images made for the whole first peak and several energy ranges are presented in Figure 2.

Figure 3 (left panel) presents an example of energy-height relation obtained for the southern footpoint and for the first HXR peak. The relation has a power-law branch which is related to purely non-thermal component in the spectrum obtained for this footpoint (Figure 3, right panel). In low energies we observe thermal sources which are located at the same altitude. Such shape of the energy-height relation is not typical. Usually we observe only a non-thermal component without significant flat part in low energies (Mrozek, 2006). With the use of power-law branch of energy-height relation we can derive the column density (N) since it is related to stopping energy of non-thermal electrons (Brown *et al.*, 2002).

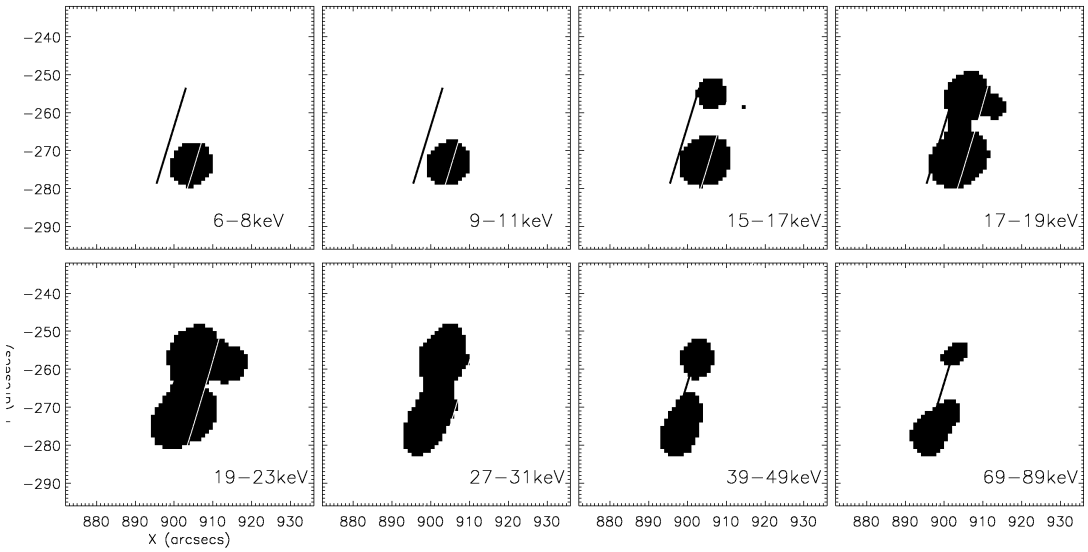

Figure 2: Maps of the 3 Aug 2002 flare obtained for time interval 19:04:35 – 19:04:47 UT in several energy bands listed in the lower right corner of each panel. Solar limb is marked by the grey line. Reference level for the height measurements is represented by the black line.

The accuracy of the centroid location can be estimated as follows. Each point (x_k, y_k) of the source has errors $(\Delta x_k, \Delta y_k)$ connected with the angular resolution. Bogachev *et al.* (2005) calculated how these errors propagate in the centroid location (x_0, y_0) and obtained following formula (the equation for Δy_0 is analogous):

$$(\Delta x_0)^2 = \frac{(\Delta x)^2}{n} + \frac{\sum_{k=1}^{n}(x_k - x_0)^2}{I_0 n^2} \qquad (1)$$

where Δx_0 is the error of the position of the centroid, n is the number of pixels in the source and I_0 is the integral intensity of the source. This method was used for HXT images but can be easily adopted for *RHESSI* images, assuming that the angular resolution is determined by the finest grid used for the image reconstruction.

3. Results

For one event, the flare of 3 August 2002, we were able to obtain energy-height relations for several consecutive time intervals covering the whole

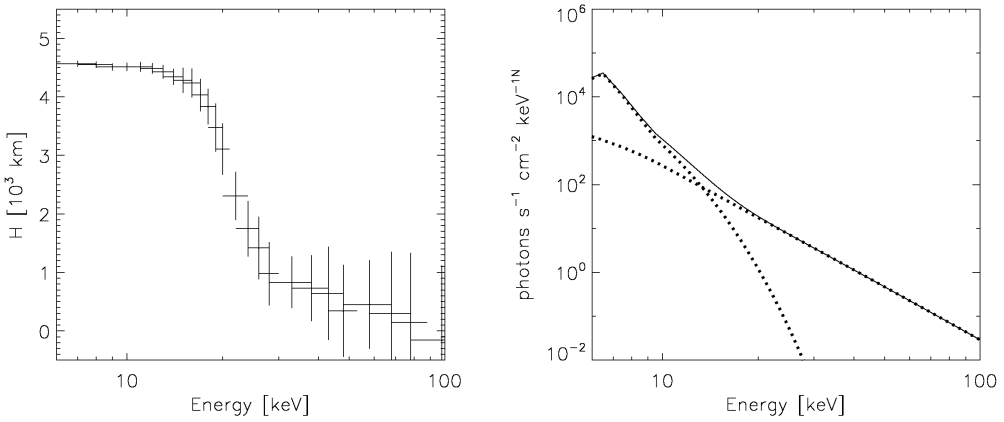

Figure 3: Left panel: The energy-height relation obtained for the southern footpoint with the use of images reconstructed for the first HXR burst. Horizontal lines represent energy intervals. Vertical lines are errors in centroid location (see the text for details). Right panel: spectrum of the southern footpoint obtained for the same time interval. Thermal and non-thermal components are represented with dotted lines.

first peak. The result is presented in Figure 4. We observed that basic characteristics of the energy-height relation are changing with time. During the observed hard X-ray burst the steep branch moves up (Figure 4). We treated this effect as some evidence of a systematical change in the density due to the chromospheric evaporation. Energy deposited by electrons in the transition region and the chromosphere was high enough to produce the pressure gradient leading to the evaporation. Due to this process the column density changes and we observe that electrons with similar energy are stopped at higher levels in consecutive time intervals.

We estimated the velocities of the observed density changes by subtracting energy-height relations obtained for consecutive intervals. For this purpose we utilized five energy-height relations starting from the relation obtained for interval 19:04:11–19:04:23. The example of the velocity-energy relation is presented in the Figure 5. This is not exactly the velocity of the moving plasma, but rather the velocity of changes in the chromosphere and transition region density structure. The obtained values are between -50 km/s and 150 km/s. Such a range of values suggests that during the impulsive phase we observe simultaneously upflows in the chromosphere and downflows in the transition region.

Negative values of velocity were observed for the low-energy, flat part of

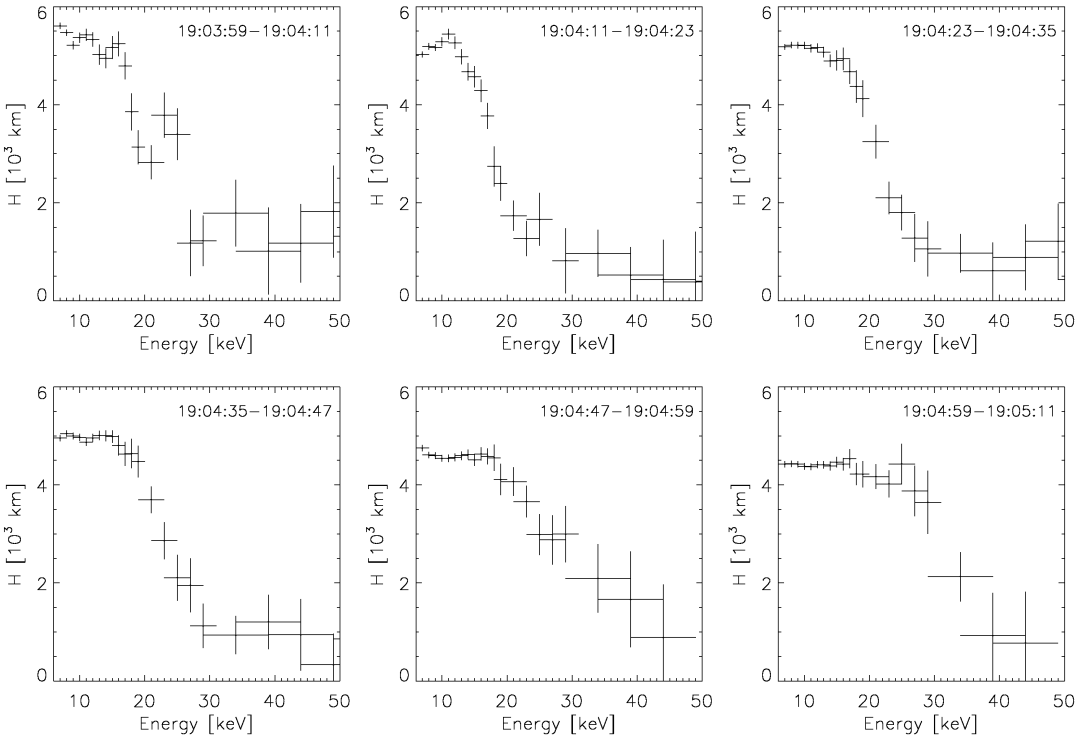

Figure 4: Energy-height relations obtained for six consecutive time intervals listed in the upper right corner of each panel.

the energy-height relation. This part is purely thermal, what was confirmed by *RHESSI* spectra obtained directly from images. This type of behaviour is rather surprising since we expect upflows in the low corona and transition region. There are two possible explanations of this observation. The first is based on the momentum deposited by non-thermal electrons. Reale *et al.* (1985) showed that the beam momentum exceeds significantly the gas pressure in the injection site. Observed downward velocities could be a manifestation of the plasma compression caused by the non-thermal electron beam. However, negative velocities are observed for the time interval 19:04:59–19:05:11 during which there is no significant non-thermal emission. Thus, we need to consider the other mechanism. Nagai and Emslie (1984) modelled the atmospheric response to the non-thermal electron beam and showed that during the impulsive phase a hot, thermal front occurs in the high chromosphere. It propagates downward with velocities of $10-30$ km/s. Due to the high density gradient in this region and due to high temperatures (low radiative losses) we expect that the emission in this region should be

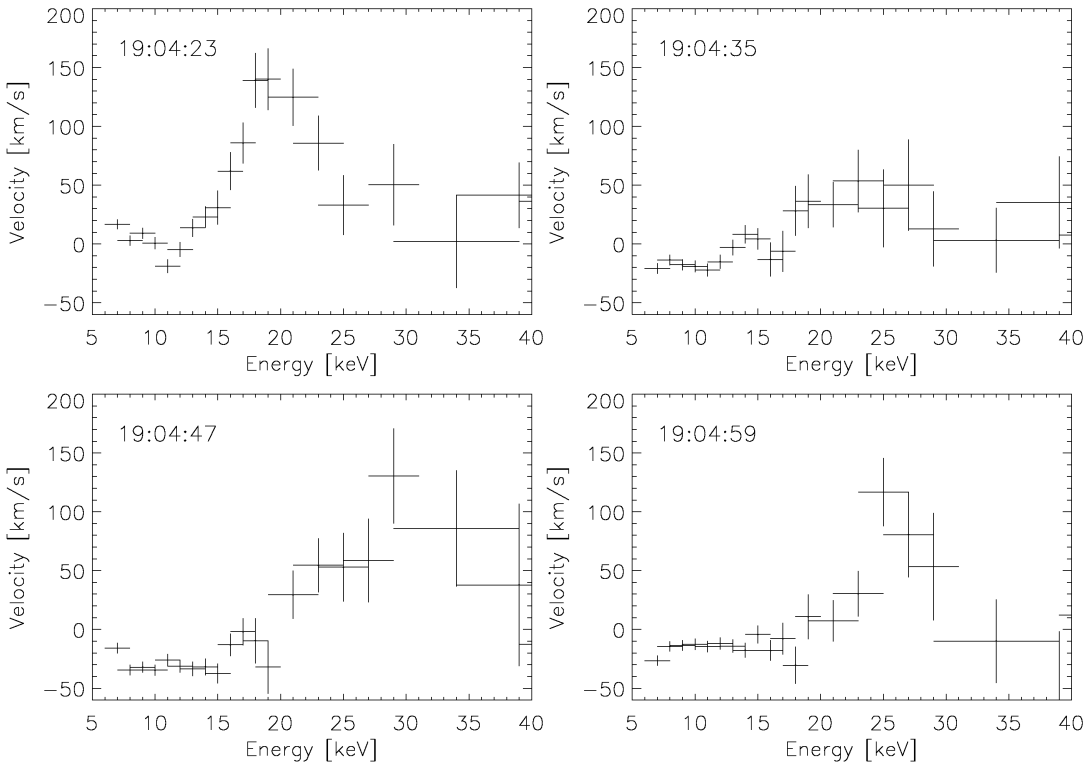

Figure 5: The velocity-energy relations obtained for four consecutive time intervals. Moment in time related to the centre of interval is listed in the upper left corner of each panel. See text for further details.

shifted downward as the thermal front propagates. In such a case there is no downward plasma motion, but only thermal energy propagation to the lower altitudes.

During the analysed burst of HXR emission we observed moving sources, but only within the chromosphere. However, above this layer, there are no significant upflows which can be treated as typical observation of the chromospheric evaporation. It is possible that the evaporation is held by the pressure caused by the deposition of the non-thermal electrons momentum. This phenomenon can be a reason why we do not observe significant plasma blobs moving from the footpoint to the loop-top kernel. To verify this hypothesis we made a set of images in several energy ranges and 4-s cadence covering the time interval of 19:05:20-19:07:20 UT. In each energy range we observed a source moving from the south footpoint to the loop top. The example of the centroid altitude measurements along the loop for several

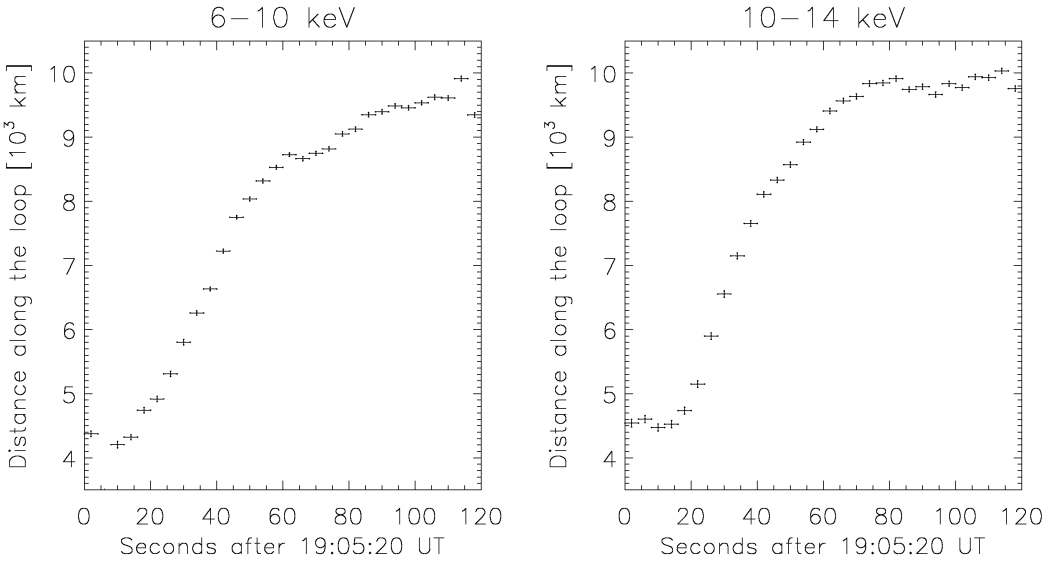

Figure 6: Velocities estimated for a source moving from southern footpoint to the loop top. This source was observed in the time interval 19:05:40–19:06:40.

time intervals is presented in Figure 6. We show only two energy intervals, but such behaviour was observed for each interval from 6 to 25 keV. Velocities were calculated for the time interval 19:05:40 – 19:06:20 in which we observed almost a linear change of location with time. Obtained values, about 150 km/s, are typical for chromospheric evaporation.

Energy-height relations obtained for several time intervals can be used for analysing the mass motion between several levels of the chromosphere. The energy of an electron stopped at a given altitude is related to the column density, thus we are able to analyse the column density changes. Moreover, if we compare the column density for neighbouring levels obtained in two different moments in time we can calculate the mass amount transferred between these levels. Taking into consideration the two moments related to the start and the end of the main peak, we estimated the mass pushed upward to be equal to 5×10^{13}g. We tried to compare this value with the additional mass which was detected in the flare loop-top kernel. It might be done in two ways. First, we calculated the emission measure, ϵ, in the coronal source before and after the main peak. Comparing these two values of ϵ we estimated the additional mass in the kernel to be about 8×10^{13}g. Second, we used scaling laws showed by Preś and Kołomański (2007) which give the relation between the geometrical and physical parameters of kernels

observed by *Yohkoh* SXT. From these scaling laws the mass contained in the kernel is equal to 3×10^{14}g. The difference between these two estimations of kernel mass is obvious, since SXT is more sensitive to the dominating, cooler (about 10 MK) component of the kernel plasma (Kępa *et al.*, 2005). There is less mass evaporated from the southern footpoint than mass contained in the loop-top kernel. Nevertheless, it is obvious that mass was evaporated also during the next two HXR bursts. Moreover, the same process took place in the second footpoint. Taking this into consideration we conclude that chromospheric evaporation provides enough mass to fill the loop-top kernel.

4. Conclusions

In this paper we presented the new method of investigating plasma dynamics in the chromosphere, transition region and lower corona. It is based on the analysis of the temporal evolution of the energy-height relation. It directly comes from the relation between the energy of the non-thermal electrons and column density needed to stop them. Treating non-thermal electrons as a tool we are able to obtain useful information about plasma distribution and its change inside the southern footpoint of the flare of 3 Aug 2002.

During the main HXR burst we observed sources moving simultaneously downward and upward in the chromosphere and transition region. In the chromosphere we observed upflows with velocities in the range of 50–150 km s^{-1}. These velocities reveal changes of the density structure in the chromosphere. Moreover, we observed a hot, thermal source which moves downward. Such an effect is predicted by theoretical models when a high-temperature front propagates downward.

The plasma blob moving above the transition region was observed after the end of the main HXR peak. Estimated velocity was in the range of 100–150 km/s which is consistent with recent results obtained by Milligan *et al.* (2003). It is significant that such behaviour was observed after the end of HXR burst. Thus, we cannot exclude that the non-thermal electron beam i.e. their momentum, may hold the chromospheric evaporation.

Detailed analysis of chromospheric evaporation leads us to the conclusion that the mass transferred up to the loop from the footpoint is in agreement with the mass contained in the flare loop-top kernel.

Acknowledgements

First, we wish to thank the *RHESSI* Team. We acknowledge many useful and inspiriting discussions of Professor M. Tomczak. We also thank Barbara Cader-Sroka for valuable remarks which led to improvement of this paper. This investigation has been supported by grant No. N203 001 32/0036 from the Polish Committee for Scientific Research (KBN).

References

Aschwanden, M.J., Brown, J.C., and Kontar, E.P.: 2002, *Solar Phys.* **210**, 383.

Bogachev, S.A., Somov, B.V., Kosugi, T., and Sakao, T.: 2005, *Asrophys. J.* **630**, 561.

Brown, J.C.: 1973, *Solar Phys.* **31**, 143.

Brown, J.C., Aschwanden, M.J., and Kontar, E.P.: 2002, *Solar Phys.* **210**, 373.

Delaboudiniére, J.-P. *et al.*: 1996, *Solar Phys.* **162**, 291.

Fisher, G.H., Canfield, R.C., and McClymont, A.N.: 1985, *Astrophys. J.* **289**, 425.

Handy, B.N., Acton, L.W., and Kankelborg, C.C.:1999, *Solar Phys.* **187**, 229.

Högbom, J.A.: 1974, *Astron. Astrophys.* **15**, 417.

Kępa, A., Sylwester, J., Sylwester, B., Siarkowski, M., and Kuznetsov, V.: 2005, *Proc. of the 11th SPM* **ESA SP-600**, 87.1.

Li, H., You, J., and Du, Q.: 2006, *Solar Phys.* **235**, 107.

Lin, R.P. *et al.*:2002, *Solar Phys.* **210**, 3.

Matsushita, K., Inda, M., and Yaji, K.: 1992, *Publ. Astron. Soc. Jpn.* **44**, L89.

Milligan, R.O. *et al.*: 2006, *Astrophys. J.* **638**, L117.

Mrozek, T.: 2006, *Adv. Space Res.* **38**, 962.

Mrozek, T. and Tomczak, M.: 2004, *Astron. Astrophys.* **415**, 377.

Nagai, F. and Emslie, A.G.: 1984, *Astrophys. J.* **279**, 896.

Preś, P. and Kołomański, S.: 2007, this issue.

Reale, F., Peres, G., and Serio, S.: 1985, *Astron. Astrophys.* **152**, L5.

Tomczak, M.: 1999, *Astron. Astrophys.* **342**, 583.